AIP | Journal of Applied Physics

The electronic structure of co-sputtered zinc indium tin oxide thin films

Paz Carreras, Sebastian Gutmann, Aldrin Antony, Joan Bertomeu, and Rudy Schlaf

Citation: J. Appl. Phys. **110**, 073711 (2011); doi: 10.1063/1.3647780
View online: http://dx.doi.org/10.1063/1.3647780
View Table of Contents: http://jap.aip.org/resource/1/JAPIAU/v110/i7
Published by the American Institute of Physics.

The electronic structure of co-sputtered zinc indium tin oxide thin films

Paz Carreras,[1] Sebastian Gutmann,[2] Aldrin Antony,[1] Joan Bertomeu,[1] and Rudy Schlaf[3,a)]
[1]*Departament de Física Aplicada i Òptica, Universitat de Barcelona, 08028 Barcelona, Spain*
[2]*Department of Chemistry, University of South Florida, Tampa, Florida 33620, USA*
[3]*Department of Electrical Engineering, University of South Florida, Tampa, Florida 33620, USA*

(Received 29 July 2011; accepted 31 August 2011; published online 12 October 2011)

Zinc indium tin oxide (ZITO) transparent conductive oxide layers were deposited via radio frequency (RF) magnetron co-sputtering at room temperature. A series of samples with gradually varying zinc content was investigated. The samples were characterized with x-ray and ultraviolet photoemission spectroscopy (XPS, UPS) to determine the electronic structure of the surface. Valence and conduction bands maxima (VBM, CBM), and work function were determined. The experiments indicate that increasing Zn content results in films with a higher defect rate at the surface leading to the formation of a degenerately doped surface layer if the Zn content surpasses ~50%. Furthermore, the experiments demonstrate that ZITO is susceptible to ultraviolet light induced work function reduction, similar to what was earlier observed on ITO and TiO_2 films. © *2011 American Institute of Physics*. [doi:10.1063/1.3647780]

INTRODUCTION

Transparent conductive oxides (TCOs) have attracted considerable attention in recent years due to their high conductivity, high transparency, and industrial process compatibility.[1,2] In solar cells, TCOs are used as transparent electrodes where band alignment matching with active layers is important. Binary compounds like doped indium oxide, zinc oxide, and tin oxide are widely used because they present unique electrical and optical properties. Zinc indium tin oxide (ZITO) alloys have been previously studied and improvements in electrical[3,4] and mechanical[5] properties compared to indium tin oxide (ITO) were reported for certain compositions. The objective of the presented experiments was to characterize the electronic structure (i.e., work function and band edge energies) of ZITO thin films in order to assess their suitability for electrode applications.

In the presented experiments, six ZITO thin films ranging from 17% to 67% Zn concentration, as well as pure ITO and ZnO films, were investigated with x-ray and ultraviolet photoemission spectroscopy (XPS, UPS). The presented results indicate the formation of a degenerately doped surface layer for ZITO films with 50% Zn or higher. This surface layer is caused by an increasing O defect density with increasing Zn concentration.

A secondary focus of the experiments was directed towards the investigation of the measurement technique itself, in particular, the UPS measurements which are the "standard" way to characterize the work function of surfaces since absolute values can be obtained with this technique. However, recent research demonstrated that UPS measurements on metal oxide surfaces can result in a lowering of the work function caused by the measurement itself.[6–9] These experiments suggested that this phenomenon is likely caused by the formation of a surface dipole due photochemical hydroxylation of the surface by UV photons during the UPS measurement. While the artifact occurs instantaneously during UPS characterization (i.e., cannot be detected by UPS itself), it was possible to identify its magnitude through low intensity x-ray photoemission spectroscopy (LIXPS), which exposes the surface only to magnitudes lower photon fluxes, while still enabling the determination of the work function. Hence, another objective of the presented research was to investigate whether ZITO surfaces are also prone to this artifact. In this context, LIXPS measurements were performed on all of the investigated films prior to the standard UPS measurement. These experiments demonstrated that ZITO films indeed show a comparable work function reduction as was seen on other *ex-situ* cleaned metal oxide surfaces.

EXPERIMENTAL

ZITO samples were deposited at the University of Barcelona by radio frequency (RF) magnetron co-sputtering of ZnO and ITO (In_2O_3 doped with 10% SnO_2) at room temperature. The equipment used was an ATC ORION sputtering from AJA International, Inc. A Zn content ratio from 0 to 67% was achieved by increasing ZnO RF power from 0 to 150 W while keeping ITO RF power constant (50 W). A pure ZnO sample was also deposited at 120 W. The sample to substrate distance was kept at 12 cm with a rotation speed of 10 rpm and 3-inch target purity was of 99.995% for ZnO and 99.99% for ITO. This process yielded ~210 nm thick films on Corning glass (1737 F). More detail about the sample preparation process can be found in Ref. 10. After deposition, the sample conductivity was measured by four-point probe to ensure identical conductivity to the samples investigated in Ref. 10.

Photoemission spectroscopy characterization was performed in a commercial ultra high vacuum (UVH) multichamber system (SPECS GmbH) at the University of South Florida. 1 cm × 1.5 cm sections of the ZITO coated glass slides were directly screwed to sample holders ensuring

a)Author to whom correspondence should be addressed. Electronic mail: schlaf@usf.edu.

electrical contact through the mounting screws. All samples were cleaned in an ultrasonic bath for 10 min each in acetone and isopropanol just before loading them into the vacuum system. No other cleaning treatment was performed in order to achieve a similar surface condition as used at the University of Barcelona lab for device preparation and characterization.

The samples were characterized with XPS (Mg Kα, 1253.6 eV) and UPS (He I, 21.21 eV). Additional LIXPS measurements were performed before and after each UPS measurement to investigate the occurrence of UV-induced work function lowering during UPS measurements. During LIXPS measurements, the X-ray gun is operated in stand-by mode, resulting in a photon exposure orders of magnitude lower compared to XPS or UPS, while still allowing the measurement of a well-resolved secondary edge. This allows the determination of the work function of the sample prior to UV exposure during UPS measurements. More details of the technique are described in Ref. 8. During UPS and LIXPS measurements, a −15 V bias voltage was applied to the sample to separate sample and analyzer spectral cutoffs. Analysis of the photoelectrons was performed with a SPECS Phoibos 100 hemispherical analyzer. The spectrometer was calibrated to yield the standard Cu $2p_{3/2}$ line at 932.66 eV and Cu $3p_{3/2}$ at 75.13 eV. Spectral analysis was done using IGOR pro software (Wavemetrics, Inc.) where work function values were determined by determining the intersect of secondary edge with the baseline of the spectra. 0.1 eV was added to such determined values to account for the analyzer broadening.[11]

The measurement protocol for all samples had four steps: An initial LIXPS characterization was carried out ("LIXPS A") to measure the work function. Then, the sample was characterized with UPS. After the UPS measurement, a second LIXPS measurement ("LIXPS B") was performed to investigate whether UPS caused any surface modification affecting the work function. Finally, each sample was characterized with XPS to assess the stoichiometry of the surface.

RESULTS

Eight samples were characterized: Pure ITO and ZnO thin films, and ITO films with 17, 37, 49, 54, 63, and 67% Zn (relative to the In content). Fig. 1 summarizes the results from the UPS measurements on this set of samples. The bottom spectra correspond to the pure ITO film, while the subsequent spectra reflect the films with increasing Zn content, with the top spectra corresponding to the pure ZnO film.

The center graph shows the raw UP-spectra as measured. The main spectral features include the Fermi energy at 0 eV binding energy, the valence bands density of states below ~3 eV and the secondary edge cutoff at about 17–18 eV. The valence bands spectra are shown in the graph on the right with the inelastic background removed. These spectra show that the valence bands maximum (VBM) binding energy changes depending on the Zn content. The ITO film has a VBM at 3.3 eV, while the edge shifts by about 0.8 eV to higher binding energy with increasing Zn content of the ZITO films. The pure ZnO film has a lower VBM energy similar to the pure ITO film.

The graph on the left shows the normalized secondary edge spectra measured with LIXPS before (LIXPS A) and after the UPS measurement (LIXPS B). The observed shift of the order of 0.5 eV to higher binding energy from A to B measurements is a result of the work function reduction of the surface due to UV-induced surface hydroxylation during the UPS measurement. However, it is also obvious that the initial LIXPS A cutoffs shift to a higher binding energy reflecting a real work function reduction as the Zn content increases. The work function change between ITO and ZnO is about 0.4 eV.

Fig. 2 shows the corresponding XPS spectra. The three graphs show the Zn $2p_{3/2}$, the O 1 s, and the In $3d_{5/2}$ lines measured on the eight thin films. The Zn $2p_{3/2}$ sequence shows an increase in intensity depending on the Zn content of the samples. This is in direct agreement with the attenuation of the In $3d_{5/2}$ emission line as the In content decreases correspondingly. Both lines show a shift to higher binding energy as the Zn content increases; however, the shifts are different in magnitude. The In $3d_{5/2}$ line shifts by 0.35 eV, while the Zn line exhibits a shift of 0.6 eV between the 17% and the 67% films. The Zn peak of the final ZnO film has a lower binding energy corresponding to only a 0.2 eV shift relative to the initial 17% film.

The O 1 s spectra show a complex change of their spectral features, which are composed of at least three lines. The main line at about 530.5 eV corresponds to O^{2-} bonded at fully coordinated metal sites, while the line at about 532 eV is related to sites with oxygen vacancies. The third (smaller) emission feature at about 532.6 eV is related to surface contamination (water, OH). As the Zn content increases the O vacancies related component increases its intensity, indicating a higher defect density in these films. The final pure ZnO film shows again a smaller 532 eV component. In addition to these stoichiometric changes, the lines also shift to higher binding energy similar to the two metal related lines. The shift of the low binding energy O 1 s line between pure ITO and ZnO is 0.7 eV.

The observed shift of each of the core level lines is most likely a result of both stoichiometric and doping density changes depending on the composition as well as the density of O vacancies in the films.

DISCUSSION

The evaluation of the UP- and LIXP-spectra shown in Fig. 1 yielded the work function and the VBM energy for each of the investigated films. In addition, using the recently published band gap energies for each of the investigated ZITO compositions,[10] the respective conduction bands minima (CBM) can also be estimated for each of the films. The results of this evaluation are shown in Fig. 3. The top part of the figure shows the evolution of the work function depending on the composition of the films. The solid round markers correspond to the work function values measured during the initial LIXPS step before the UPS measurement was performed on each sample. The open markers correspond to the

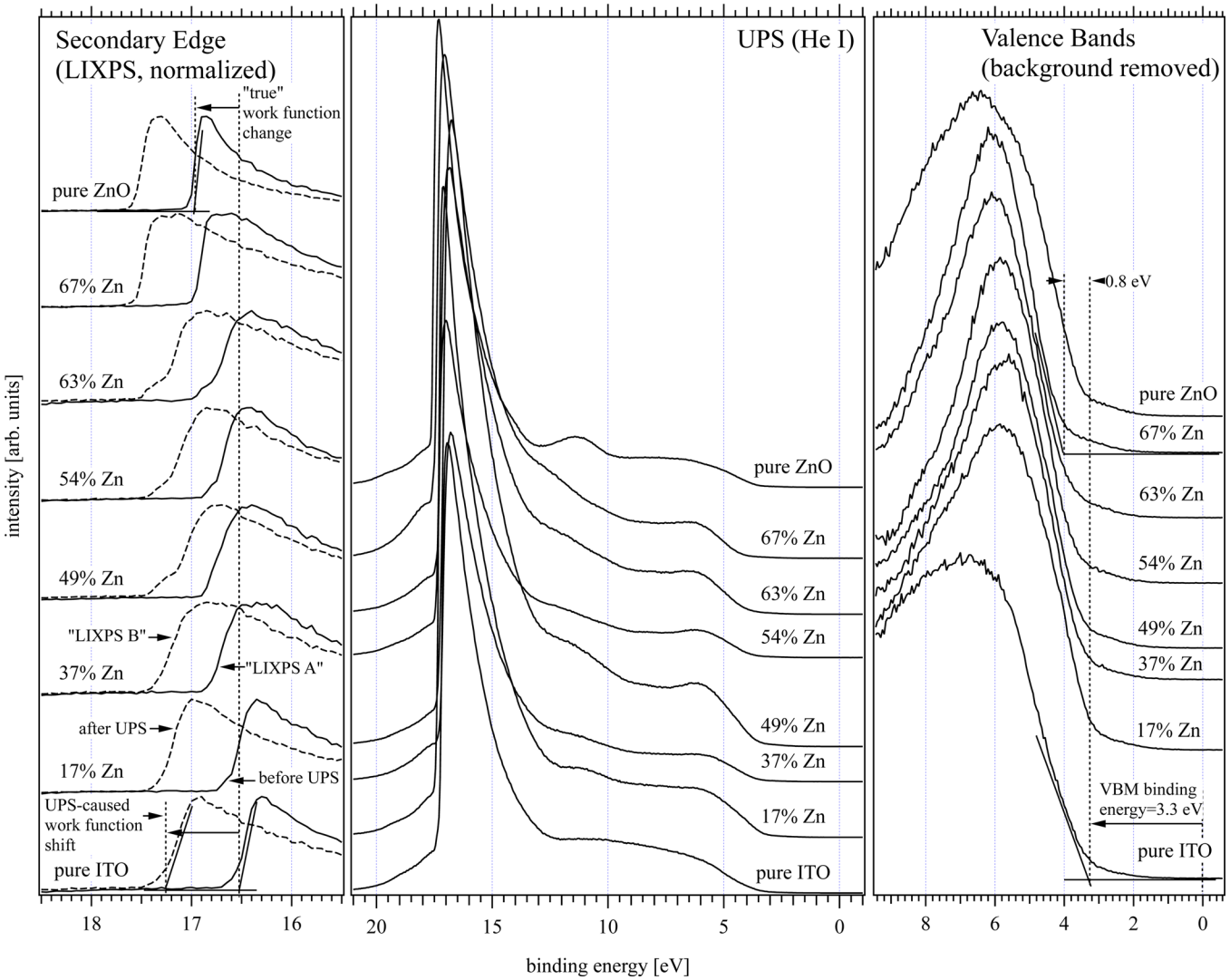

FIG. 1. (Color online) Work function and valence bands characterization. The center graph shows the raw UPS data. The strong feature at ~17 eV binding energy is the secondary edge cutoff, which allows the determination of the work function of the samples. The energy range between 0 and ~10 eV corresponds to the valence bands density of states of the samples. Part of this range is shown magnified and with the inelastic background removed on the right. A distinct change of the density of states can be observed as the Zn concentration of the films changes. Also, a shift of the VBM to higher binding energy is observed. On the left the secondary edge cutoff measured with low intensity XPS (LIXPS) before and after the UPS measurements is shown. The exposure to the UV light during UPS data collection shifts the secondary edge to higher binding energy on all samples. This corresponds to a work function lowering, which is caused by photochemical hydroxylation of the surface.

work function values determined from the second LIXPS measurement after the UPS characterization. The two dashed lines correspond to least square fitted lines into each of the two sets of values. The lines indicate that the overall work function change caused by the UPS measurement appears somewhat reduced as the Zn concentration is increased. However, the overall values in the range of ~0.4–0.6 eV are in good agreement with values previously seen for this artifact on ITO and TiO_2 surfaces.[6–9] In these previous studies, it was found that UV or x-ray photons cause a photochemical surface hydroxylation, resulting in a uniform dipole potential across the surface. This lowers the work function since the attached −OH groups are oriented with their positive hydrogen end away from the surface.

For the further evaluation of the electronic structure of the investigated films the work function values of the LIXPS A measurement will be used since they yield the "true" work function of the samples before the UPS measurement caused the work function to drop. It has been previously shown in direct comparison with *in-situ* Kelvin probe measurements that LIXPS measurements do not alter the work function significantly during the short and weak x-ray exposure needed for a single LIXPS scan.[7] Fig. 3 shows that the work function of the films drops by about 0.4 eV between pure ITO and pure ZnO. The absolute values range from 4.74 eV for pure ITO to 4.3 eV for pure ZnO.

These values fall into the range of work function values established previously for these materials. The work function value of the pure ITO sample is similar (±0.1 eV) to values previously measured on *ex-situ* cleaned thin films.[6,7,12] Scanning Kelvin probe measurements by Chen on ITO films yielded values ranging from 4.28 to 4.86 eV depending on the surface treatment.[13] Previous work function measurements on pure ZnO by Kelvin probe yielded values between

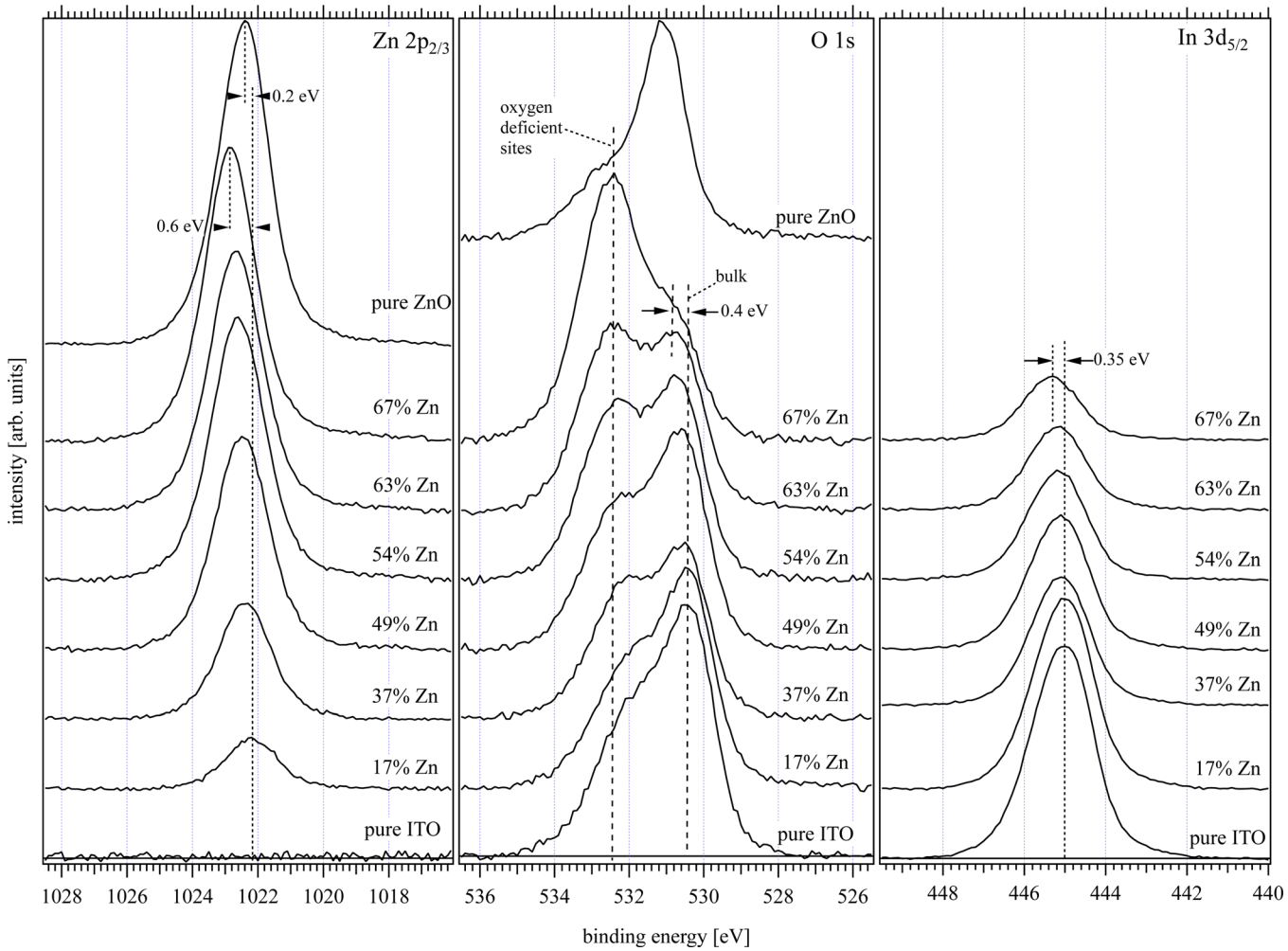

FIG. 2. (Color online) Core level photoemission spectra measured with XPS. The graph on the left shows the Zn $2p_{3/2}$ peak, which increases proportionally to the Zn concentration in the films. The center graph shows the corresponding O 1s emission features. The feature is composed of three main features related to oxygen atoms at fully coordinated metal sites (~530.4 eV), sites with oxygen vacancies (~532 eV), and in the surface contamination layer (~532.6 eV). As the Zn concentration rises in the ZITO films the vacancy-related component strongly increases in intensity, pointing towards an increased vacancy density.

4.45 and 4.50 eV,[14] similar to the presented value of 4.3 eV. Klein *et al.*[15] investigated a variety of *in-situ* deposited ZnO layers at room temperature, measuring work function values ranging from 4.3 to 5.2 eV depending on the oxygen deficiency of the films. The same paper gives values between 3.8 and 4.7 eV (Ref. 15) for *in-situ* prepared 10% Zn and 30% Sn co-doped In_2O_3, which is in good agreement with the range found here (4.4–4.7 eV). Finally, a similar range of work function values was found on Al-doped ZnO films through scanning Kelvin probe measurements.[16]

The bottom part of Fig. 3 shows a graph where the VBM and CBM energies of the films are plotted vs. the Zn concentration. The full markers show the VBM values as determined from the valence bands edge cutoff of each of the spectra shown in Fig. 1. The corresponding CBM energies were determined using the optical band gap values determined earlier on these films via UV-VIS spectroscopy.[10] The graph shows that, as the Zn concentration is increased in the ITO films, the VBM shifts to higher binding energy. This corresponds to an upwards shift of the Fermi level in the band gap. The Fermi level position is indicated as dashed line in the graph. The graph suggests that the Fermi level enters the conduction bands at the 50% concentration point. As the concentration further increases, the Fermi level advances deeper into the conduction bands. In the case of the pure ZnO film the Fermi level is again close to the CBM. This observation corresponds to the increase of the O-vacancy related O 1s peak in Fig. 2, suggesting that the defect density rises in tandem with the Zn concentration resulting in degenerate doping levels. This interpretation is supported by experimental results on ZnO surfaces where it was found that defect densities commensurate with degenerate doping levels can exist, which result in a highly conductive surface layer.[17] Additionally, recent data by Klein *et al.*,[15] where ZnO films were prepared by magnetron sputtering with varying oxygen content, demonstrated that highly oxygen deficient films show degenerate doping levels.

The question that arises from this interpretation is why the UP-spectra do not show emissions at the Fermi energy (i.e., right below 0 eV). If the Fermi level is located above the CBM, then occupied states exist directly below the Fermi level, which should be observable with photoemission spectroscopy. The absence of notable emissions can be tentatively explained by the unique band structure of ITO and

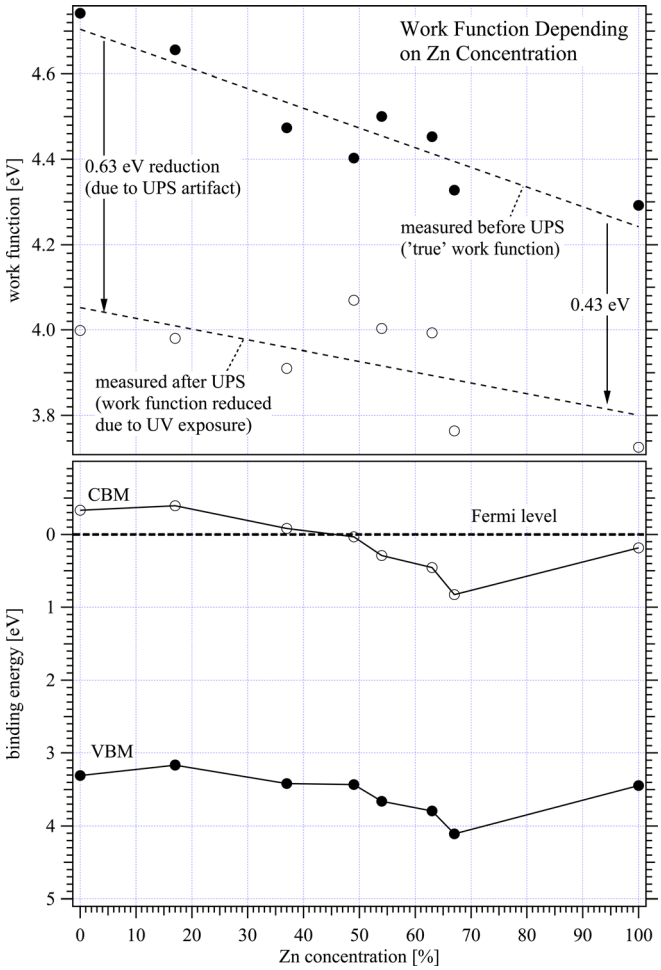

FIG. 3. (Color online) Work function values determined from the spectra shown in Fig. 1. The top graph shows the work function values derived from the LIXP-spectra measured before (full circles) and after (open circles) the UPS measurement. Generally, the work function of the films decreases as the Zn concentration rises. All samples showed a strong work function reduction between 0.63 and 0.43 eV caused by the UPS measurement. The bottom graph shows the corresponding values for the VBM binding energy (full circles) as determined from the low binding energy cutoff position of the UP-spectra. The associated CBM energies are also shown (open circles). They were calculated by using the optical band gap energy. As the Zn concentration increases the VBM binding energy increases, causing the Fermi level to enter the conduction bands (dashed line).

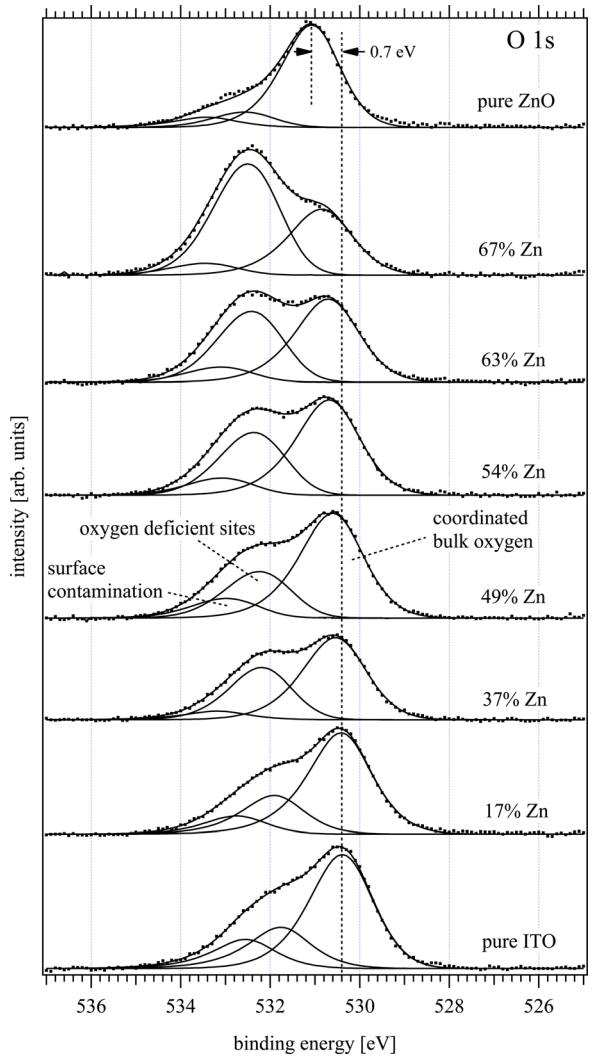

FIG. 4. (Color online) Least squares fit of the O 1s emission feature. Three individual lines were fitted reflecting oxygen atoms at fully coordinated metal sites (~530.4 eV), sites with oxygen vacancies (~532 eV), and in the surface contamination layer (~532.6 eV). The main peaks show a shift of about 0.7 eV to higher binding energy.

ZnO. Both materials (and likely their ZITO alloys—unfortunately no band structure calculations have been carried out to date for these materials) have only weakly dispersive valence bands resulting in a high density of states at the band edge. This is in agreement with the strong VBM features observed in the UP-spectra in Fig. 1. In contrast, the bottom of the conduction bands is formed by only a single band with a large dispersion.[18–21] This results in a very weak and gradual density of states onset spread over several eV. The consequence of this gradual onset is that the density of states in the relevant ~1 eV energy interval above the CBM is magnitudes lower than at the VBM, resulting in a vanishingly weak signal at the band edge. This interpretation is supported by the results of Klein *et al.*,[15] whose UPS data also did not show significant conduction bands emissions on degenerate films, and also by previous photoelectron spectroscopy measurements on single crystalline ZnO surfaces, where a VBM energy of 3.6 eV was found, while conduction band related emissions were absent.[22]

Fig. 4 shows the O 1 s emission feature fitted with three individual lines reflecting O 1s emissions related to fully coordinated metal ion sites (~530.4 eV), sites with oxygen vacancies (~532 eV), and oxygen related to environmental contaminants (~532.6 eV) present on the sample surface after the *ex-situ* solvent cleaning step (this assignment is inspired by a discussion of O 1 s spectra measured on ITO surfaces by Fan and Goodenough[23]). It is obvious that with increasing Zn concentration the oxygen vacancies related component increases strongly relative to the 530.4 eV peak. This is shown in Fig. 5 where the oxygen/metal intensity ratios are plotted for the 530.4 eV and the 523 eV peaks. The ratios are relative to the combined Zn-In metal peak intensity (except for the pure films). These curves clearly show that the oxygen deficiency rises as the Zn component is getting stronger, which is in good agreement with the concurrent Fermi level rise in the band gap determined above. It is interesting to note that the defect level is considerably lower in

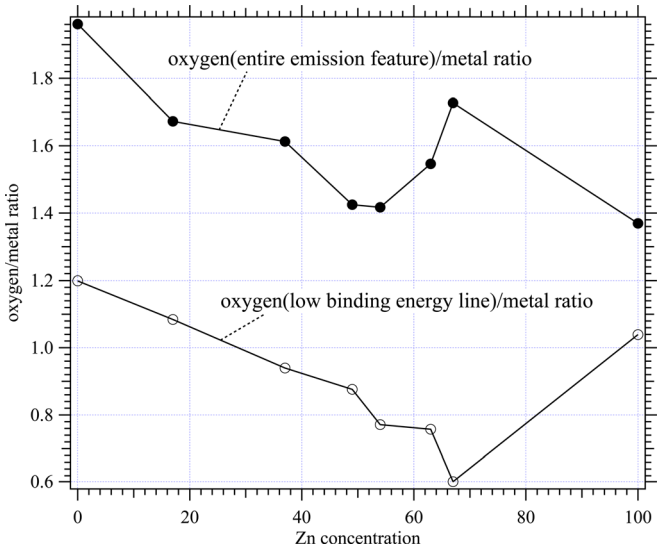

FIG. 5. (Color online) Ratio between oxygen and metal emissions depending on the Zn concentration. The lower graph (open circles) plots the ratio between the oxygen line at ~532.4 eV and the total metal atom emissions vs. the Zn concentration. It is obvious that the number of fully coordinated sites drops strongly as the Zn concentration increases. Only for the pure ZnO film the ratio recovers to a near stoichiometric value. The top graph shows the ratio between the entire O 1s feature and the metal peaks.

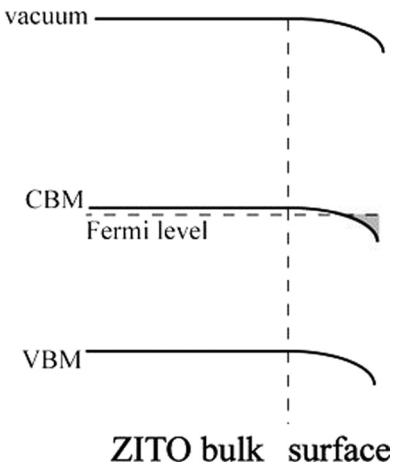

FIG. 6. Electronic structure at ZITO film surface. A high oxygen vacancy density at the surface causes the Fermi level to enter the conduction bands.

for the ZnO film, which is probably related to the fact that alloys typically have higher defect densities than their associated pure compounds. The contamination related emission component remains fairly stable throughout the experimental series, which is reasonable due to the identical cleaning procedure applied to all samples.

Peak fits to the corresponding Zn 2p and In 3d peaks revealed a constant full width at half maximum (FWHM) across the compositional spectrum. The peaks had widths of 1.9 eV for the Zn 2p peak and 1.8 eV for the In 3d line. This result is in agreement with earlier measurements on In_2O_3 and ITO films with varying O vacancy density, where the metal peaks' FWHM also remained unaffected by the stoichiometry. This was related to the presence of mobile O 5s electrons equally shared by all metal ions, which smoothens out the charge density on the metal sites.[23]

It is interesting to note that all observed core level peaks showed significant shifts to higher binding energy with increasing Zn concentration. The Zn 2 p peak shifted by 0.6 eV between 17% and 67% Zn concentration, while the In 3d peak shifted by 0.35 eV between pure ITO and the 67% ZITO film. The sample-related oxygen lines on the other hand exhibited a gradual shift from pure ITO to pure ZnO of about 0.7 eV. It is clear that part of the shift is related to the change of the average charge localized on the O and metal sites due to the changing chemical environment, and the varying oxygen vacancy density depending on the Zn concentration. A second effect that plays a role is most likely the vacancy density related Fermi-level shift into the conduction bands, which increases the binding energy of the core levels of all atomic species present in the samples.

Unfortunately, it is difficult to separate these effects since they occur simultaneously. An assessment of the binding energy changes caused by the Fermi level shift is difficult due to the associated changes in the density of states at the VBM, which makes it impossible to separate a realignment of the band edge due to a different chemical environment from a shift caused by the changing charge carrier density. Likewise, the observed core level shifts are caused by both chemical changes and Fermi level shifts.

While a full analysis therefore is not possible, a few observations can still be made. The rise of the O-vacancies related O 1s component in conjunction with increasing Zn content suggests that a majority of the O vacancies are localized at Zn sites. Hence, the difference between the Zn 2p and the In 3d shifts (0.6 eV vs. 0.35 eV) appears to be related to the changing chemistry of the Zn sites, while the 0.35 eV shift of the In 3d line can be reasoned to be related mostly to the binding energy increase due to the Fermi level shift.

From the bottom graph in Fig. 3, it is obvious that the Fermi energy relative to the VBM shifts by about 0.8 eV between pure ITO and the 67% ZITO film. Considering the 0.35 eV shift of the In 3d line, it can then be reasoned that the balance between these shifts, 0.45 eV, is actually related to a lowering of the VBM (or in other words an increase of the ionization energy) of the ZITO film. This is supported by the fact that the work function is lowered by only about 0.3 eV between ITO and 67% ZITO, which is in close agreement to the 0.35 eV In 3d shift.

The final point of this discussion focuses on a comparison of the surface related data presented here with the previous investigation of the bulk properties of these films.[10] These previous investigations yielded that the carrier density was reduced with increasing Zn content. This is in direct disagreement with the Fermi level shift into the conduction band observed here, which suggests a strong increase in the carrier density. Furthermore, it was found that the absorption edge of the ZITO alloys is reduced by about 0.4 eV between the pure ITO film and the 67% ZITO layer. The results presented here would suggest that the absorption edge of those films where the Fermi level entered the conduction bands should actually shift to larger energies (or shorter wavelengths, respectively) due to the Burstein effect[24] where occupied states at the CBM prevent transitions from the VBM to the CBM resulting in a larger apparent band gap.

The only way to explain this discrepancy is to realize that the results in Ref. 10 reflect bulk properties, while the photoemission spectroscopy data presented here relates to surface properties. This allows the conclusion that the vacancy density of the investigated ZITO films is higher at the surface than in the bulk, which gives rise to a highly conductive surface layer on top of a less conductive bulk phase. This is shown schematically in Fig. 6. The Fermi level enters the conduction band in the surface layer resulting in a thin degenerately doped layer.

CONCLUSIONS

ZITO transparent conductive thin films with varying Zn concentration were investigated with XPS, UPS. The measurements showed that with increasing Zn concentration the oxygen vacancy concentration of the surface increased, resulting in a degenerately n-doped surface layer. The work function at the same time decreased due to this effect, resulting in a lower ionization energy of the surface. Comparison with bulk optical absorption and carrier density measurements previously published allowed the conclusion that the degenerately doped region is confined to a thin surface layer. Additionally, the experiments demonstrated that the work function of *ex-situ* cleaned ZITO surfaces is reduced by about 0.5 eV during UPS measurements, similar to what was observed earlier on other metal oxide surfaces.

ACKNOWLEDGMENTS

The authors gratefully acknowledge funding by the National Science Foundation (NSF DMR 0906922), the Spanish Ministerio de Ciencia e Innovación (ENE2010-21384-C4-03), and the European Regional Development Fund through the project MICROSIL08 (PSE-120000-2008-001). Paz Carreras' stay at USF was made possible through a grant from the Generalitat de Catalunya (BE-DGR-2010).

[1]D. S. Ginley and J. D. Perkins in *Handbook of Transparent Conductors* (Springer, Berlin, 2010), pp. 1–25.
[2]H. Hosono, Thin Solid Films **515**(15), 6000 (2007).
[3]M. K. Jayaraj, K. J. Saji, K. Nomura, T. Kamiya, and H. Hosono, J. Vac. Sci. Technol. B **26**(2), 495 (2008).
[4]D.-S. Liu, C.-H. Lin, B.-W. Huang, and C.-C. Wu, Jpn. J. Appl. Phys. **45**, 3526 (2006).
[5]D. Y. Lee, J. R. Lee, G. H. Lee, and P. K. Song, Surf. Coat. Technol. **202**(22–23), 5718 (2008).
[6]R. Schlaf, H. Murata, and Z. H. Kafafi, J. Electron Spectrosc. Relat. Phenom. **120**, 149 (2001).
[7]M. M. Beerbom, B. Lagel, A. J. Cascio, B. V. Doran, and R. Schlaf, J. Electron Spectrosc. Relat. Phenom. **152**(1–2), 12 (2006).
[8]Y. Yi, J. E. Lyon, M. M. Beerbom, and R. Schlaf, J. Appl. Phys. **100**, 093719 (2006).
[9]S. Gutmann, M. A. Wolak, M. Conrad, M. M. Beerbom, and R. Schlaf, J. Appl. Phys. **107**, 103705 (2010).
[10]P. Carreras, A. Antony, R. Roldán, O. Nos, P. A. Frigeri, J. M. Asensi, and J. Bertomeu, Phys. Status Solidi C **7**(3–4), 953 (2010).
[11]J. Kohlscheen, Y. N. Emirov, M. M. Beerbom, J. T. Wolan, S. E. Saddow, G. Chung, M. F. MacMillan, and R. Schlaf, J. Appl. Phys. **94**(6), 3931 (2003).
[12]J. S. Kim, B. Lagel, E. Moons, N. Johansson, I. D. Baikie, W. R. Salaneck, R. H. Friend, and F. Cacialli, Synth. Met. **111**, 311 (2000).
[13]S.-H. Chen, J. Appl. Phys. **97**(7), 073713 (2005).
[14]K. B. Sundaram and A. Khan, J. Vac. Sci. Technol. A **15**(2), 428 (1997).
[15]A. Klein, C. Korber, A. Wachau, F. Sauberlich, Y. Gassenbauer, R. Schafranek, S. P. Harvey, and T. O. Mason, Thin Solid Films **518**(4), 1197 (2009).
[16]S.-H. Chen, C.-F. Yu, Y.-S. Lin, W.-J. Xie, T.-W. Hsu, and D. P. Tsai, J. Appl. Phys. **104**, 114314 (2008).
[17]W. Gopel and U. Lampe, Phys. Rev. B **22**(12), 6447 (1980).
[18]O. N. Mryasov and A. J. Freeman, Phys. Rev. B **64**(23), 233111 (2001).
[19]W. J. Fan, J. B. Xia, P. A. Agus, S. T. Tan, S. F. Yu, and X. W. Sun, J. Appl. Phys. **99**(1), 013702-4 (2006).
[20]A. R. H. Preston, B. J. Ruck, L. F. J. Piper, A. DeMasi, K. E. Smith, A. Schleife, F. Fuchs, F. Bechstedt, J. Chai, and S. M. Durbin, Phys. Rev. B **78**(15), 155114 (2008).
[21]R. M. Balabai and P. V. Merzlikin, Ukr. J. Phys. **55**(10), 1128 (2010).
[22]R. T. Girard, O. Tjernberg, G. Chiaia, S. Soderholm, U. O. Karlsson, C. Wigren, H. Nylen, and I. Lindau, Surf. Sci. **373**(2–3), 409 (1997).
[23]J. C. C. Fan and J. B. Goodenough, J. Appl. Phys. **48**(8), 3524 (1977).
[24]E. Burstein, Phys. Rev. **93**(3), 632 (1954).